Proceedings of the 28th IEEE
EMBS Annual International Conference
New York City, USA, Aug 30-Sept 3, 2006

Towards an Automatic Coronary Artery Segmentation Algorithm

Pascal Fallavollita, and Farida Cheriet, *Members, IEEE*

Abstract— **A method is presented that aims at minimizing image processing time during X-ray fluoroscopy interventions. First, an automatic frame extraction algorithm is proposed in order to extract relevant image frames with respect to their cardiac phase (systole or diastole). Secondly, a 4-step filter is suggested in order to enhance vessel contours. The reciprocal of the enhanced image is used as an alternative speed function to initialize the Fast Marching Method. The complete algorithm was tested on eight clinical angiographic data sets and comparisons with two other vessel enhancement filters (Lorenz and Frangi) are made for the centerline extraction procedure. In order to assess the suitability of our filter the extracted centerline coordinates are compared with the manually traced axis.**

I. Introduction

Coronary heart disease (CHD) is the single leading cause of death in America today and it accounted for 494,382 of all deaths in the United States in 2002, while in Canada the same year 74,626 Canadian deaths had occurred [1]. CHD is caused by atherosclerosis, the narrowing of the coronary arteries due to fatty build-ups of plaque. This leads to artery stenosis and it is likely to produce heart attack, angina pectoris (chest pain) or both. Fluoroscopic imaging is the method of choice for interventionists for proper diagnostic of CHD. In most cases they are also able to look at a 3D computer model of the diseased coronary artery. To arrive at this model, it is imperative that excellent segmentation and automated techniques for 2D fluoroscopic image analysis be developed.

Many methods have been described (see: [2]–[6]) for the segmentation of the central axis of an artery. Hessian-based vessel enhancement filters have been proposed by Lorenz et al. [2], and Frangi et al. [3]. Authors in [4] and [5] assume vessels are tubular structures and that relevant information can be obtained by extracting 2nd order derivatives at multiple scales by inspecting the modes of variation of a Hessian matrix. In terms of the Fast Marching Method (FMM) approaches, defining a speed function is crucial in path extraction, since the extracted path is a minimum-cost path of the specific cost selected. For a non-trivial path extraction problem, such a cost is often difficult to define. In [6], the cost image was defined as the reciprocal of the vessel-enhanced image. When extracting guidewires or line-like objects, enhancing the X-ray image using non-maximum suppression and a salience distance transform produced a successful cost image [7].

However, some discrepancies between the segmentation and the real vessel tree still persist. A major difficulty is that vessels can be broken into several disconnected components and that discontinuities may occur at bifurcation or stenosis points. The work in this paper is an extension of traditional two-click fast marching methods and it started by applying the method proposed by Olabarriaga et al. The method compares some vessel enhancement techniques on CT images. The cost image was derived from these techniques in order to extract the center axis of the artery. Although we are using only fluoroscopic images in our study, our motivation to apply Olabarriaga's cost image method is that is simple, efficient and it has been successfully adopted in other modalities such as Magnetic Resonance (MR), and used on other vessel types such as the carotids and aorta. In our study, we introduce two minor modifications to the method in [6]. First, in order to avoid ECG synchronization with our angiographic data, we propose a simple technique to extract important images that fall in the diastolic and systolic phases of the cardiac cycle. Secondly, we introduce an alternative filter in order to enhance the main coronary artery present in the 2D image. The cost function will still be defined as the reciprocal of this vessel enhanced image. Our extracted centerline will be compared to the ones obtained using the Frangi and Lorenz methods. Final results are evaluated and compared based on reference paths traced manually on the fluoroscopic images. The objective of this work is to investigate and compare the capabilities of our algorithm in order to eventually arrive at a fully automated central axis segmentation tool when analyzing only fluoroscopic images.

II. Methodology

A. Automatic Extraction of Images

Traditionally, ECG-based timing ensures a proper match of the image data with the respective heart phase. This ensures that important images in the diastolic or systolic phases can be analyzed. So as to minimize motion blur and extract relevant images, we developed the following method to select the image frame to be analyzed during the vessel enhancement and centerline extraction process. The

Manuscript received April 24, 2006. This work was supported in part by NSERC (Natural Sciences and Engineering Research Council).

P. Fallavollita. Ph.D student, Institute of Biomedical Engineering, École Polytechnique de Montreal, C.P. 6079, 53851 succ. Centre-ville, Montreal, H3C 3A7, Canada. Phone: (514) 340-4711 ext: 5057. (e-mail: pascal.fallavollita@polymtl.ca).

F. Cheriet. Associate Professor, Department of Computer Engineering, École Polytechnique de Montreal, C.P. 6079, 53851 succ. Centre-ville, Montreal, H3C 3A7, Canada. (email: farida.cheriet@polymtl.ca)

algorithm calculates the standard deviation of the differences between all the pixels of two successive frames in an entire angiographic sequence. The feasibility of having the diastole or systole frames extracted a priori without recording electrocardiogram information is valuable and would save time throughout the data analysis.

B. 4-Step Vessel Enhancement Filter

A homomorphic filter is first used to denoise the fluoroscopic image. The homomorphic filter tends to decrease the contribution made by the low frequencies and amplify the contribution of high frequencies. The result is simultaneous dynamic range compression and contrast enhancement. Once implemented, the user will select a cutoff frequency and assign a value for the ratio between the high frequencies and low frequencies as defined in [8].

Secondly, the Perona-Malik anisotropic diffusion method was then implemented in order to reduce and remove both noise and texture from the fluoroscopic image, as well as, to preserve and enhance structures [9]. The anisotropic diffusion process is presented as follows:

$$\frac{\partial \rho}{\partial t} = \nabla \cdot (D \nabla \rho) \qquad (1)$$

where D is the diffusion coefficient and the concentration gradient is given by $\nabla \rho$. This equation states that the rate of change in concentration is proportional to the divergence of the flux over a period of time, t. Two constants will be selected: κ_{aniso} controls conduction as a function of the gradient; and λ_{aniso} will control the speed of diffusion.

The third step in our vessel enhancement procedure involves using a shock filter. The shock filter results in a robust and stable deblurring process that can still be effective in noisy environments, such as in fluoroscopy, due to the low signal to noise ratio of this type of imaging modality. Gilboa et al. [10] have recently developed a filter coupling shock and linear diffusion. To regularize the shock filter, the authors suggest adding a complex diffusion term and using the imaginary value as the controller for the direction of the flow instead of the second derivative. The complex shock filter is given by:

$$I_t = -\frac{2}{\pi} \arctan\left(a \operatorname{Im}\left(\frac{I}{\theta}\right)\right) |\nabla I| + \lambda I_{\eta\eta} + \tilde{\lambda} I_{\xi\xi} \qquad (2)$$

where a is a parameter that controls the sharpness of the slope, $\lambda = re^{i\theta}$ is a complex scalar, $\tilde{\lambda}$ is a real scalar, $\xi\xi$ is the direction perpendicular to the gradient and $\eta\eta$ is the direction of the gradient.

Morphological filtering was applied as a final image-processing step in order to eliminate background elements around the main coronary artery. The structuring element will suppress the background (black) and enhance the artery (grayscale). We chose a disk-structuring element with a specified pixel radius since the contour of the coronary artery can be modeled as a collection of disks varying slowly at a given radius, and its centerline is the union of the centers of these disks.

C. Minimum Cost Path

As in [6], the speed function used to initialize the FMM will be equivalent to the reciprocal of our vessel-enhanced image using our 4-step filter. It is the fourth step of the filter (morphological) that will permit the cost image to have a high cost for background pixels, and a low cost for vessel pixels. When using the FMM, if the cost is only a function of the location x in the image domain, then the cost function is called isotropic. Hence, if the cost function is isotropic, the arrival time map U satisfies the Eikonal equation. It is to note that in the isotropic case, the fastest way of traveling always occurs along the direction that is perpendicular to the wave front. The shifted-grid 8-neighbor FMM, as presented in [7], is used to extract the center axis of the artery in our study. The FMM worked well for line-like structures and we deemed it reasonable to attempt it on tubular structures (coronary arteries) as well. The cost will be defined at the center (or inside) of four pixels and the arrival time will be computed at the four pixel nodes. The arrival time value assigned is the smallest value of the eight neighbors. The updating step after accepting point x is given in [7] and omitted here for brevity. The gradient descent method is used for path extraction. Two-clicks are required by the user to extract the centerline.

D. Evaluation

We tested our proposed method on eight angiographic image datasets. Image sizes were 512 x 512 pixels. Our automatic image extraction technique was implemented first. At most, three cardiac cycles were present in all datasets. The extracted images were then normalized and then vessel enhanced using the 4-step filter discussed in the previous section. Eight principal arteries were identified with lengths $\in$ [140,240] pixels and their central axes were manually traced. We then implemented the Lorenz and Frangi filters, adapted to 2D images, using their respective equations as outlined in [6]. The response at different scales can be combined by taking the maximum response over a range of scales. Hence, ten scales were used, $\sigma \in$ [0.25, 2.5] pixels. The center axis of the eight principal arteries was extracted with the FMM using as cost images the reciprocal of the Lorenz, Frangi and 4-step filter. The parameter configuration for each filter was determined empirically by ensuring that the principal artery was visible. The parameter values are: Lorenz: η = 1 (normalizes responses across all scales), Frangi: β = 3 (control value to discriminate blob-like structures), γ = 5 (control value to eliminate background noise), 4-step filter: *cutoff frequency*= 0.1, *ratio* =2

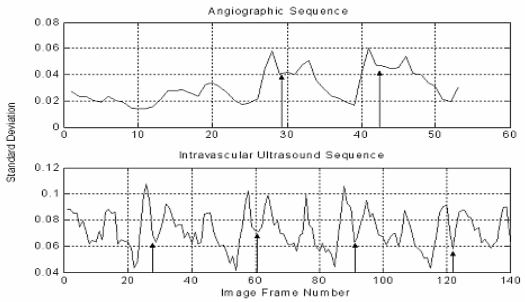

Fig. 1. Automatic image extraction method on an angiographic sequence (top) and an IVUS sequence (bottom). The minimum peaks (smallest standard deviation) in both figures corresponded to diastolic phases. The first maximum peak is then observed, followed by a first minimum point, which corresponds, to the systolic phase (showed by arrows).

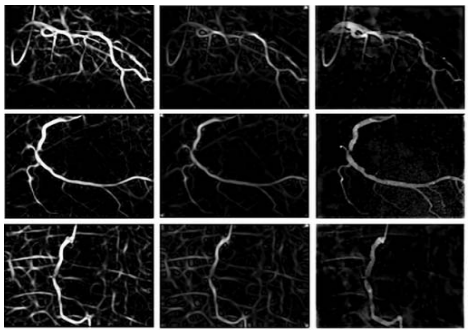

Fig. 2. Vessel enhancement filtering on three angiographic images using the Frangi (left column), Lorenz (center) and 4-step filter (right column). The coronary artery contours for the Lorenz filter appear to be slightly smaller than their true size with respect to the two other filters.

(homomorphic), $\kappa aniso$= 0.05, $\lambda aniso$= 0.05 (anisotropic diffusion), λ = 0.1, $\tilde{\lambda}$ = 0.2, a= 0.3, θ= pi/1000 (complex shock), and *radius*=10 pixels (morphological). The number of iterations was set to 20 for both the anisotropic diffusion and shock filter phases. Results are evaluated based on an error measure corresponding to the distance *D(t)* between all points in the automatic path *FMM(t)* and the reference path *Ref(s)* computed as follows:

$$D(t) = \min_{s} \left| \mathrm{FMM}(t) - \mathrm{Ref}(s) \right| \qquad (3)$$

The mean distance is used for general quality assessment.

III. Results and Discussion

In Fig. 1, we visualize the results obtained using our automatic extraction algorithm on: (top) an angiographic sequence containing 52 frames having two minimum peaks roughly located at frame numbers 24 and 38, (bottom) an intravascular ultrasound sequence (IVUS) containing 140 frames, at 30 frames per second, having four minimum peaks roughly located at frame number 21, 55, 85, 115. The minimum peaks corresponded to the smallest standard deviation and by visualizing the image frame and its neighborhood we confirmed that the image corresponded to

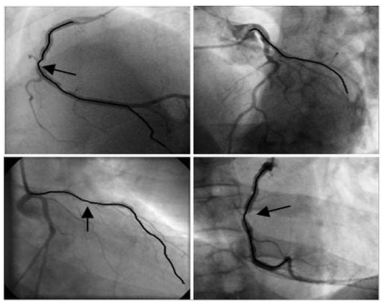

Fig. 3. Centerline extraction results on four angiographic images using our proposed 4-step filter and FMM method. The centerlines are superimposed on the original diastolic fluoroscopic images. Arrows point to stenosis locations.

the diastolic phase. The maximum peak immediately following the diastole minimum corresponds to the heart movement. This maximum peak is followed by a first minimum peak (the contractile phase in systole). We then investigated the quality of the images. Visual inspection of the extracted systole and diastole images confirmed that the image with the least motion blur occurred in the diastolic phase. In each of our eight data sets we were able to distinguish the diastolic frame correctly after the contrast agent was inserted into the artery. The use of the IVUS sequence was important to establish a set of conditions that will allow proper functioning of our method. If the images are very noisy or the disparity between images is too high, it is possible to not identify the first systolic frame correctly, after contrast agent insertion. This was a main reason why extracting the systolic phase was more of a challenge. We were able to extract the first systolic frame in only four of the eight datasets. This is because in certain cases we observed two maximum peaks adjacent to each other following diastole. There was no minimum that followed these maximum locations. Subsequent systolic images were extracted in the second or third cardiac cycle where visually possible on the standard deviation plot.

In all eight data sets, we were able to extract the principal coronary artery contours (see Fig. 2) and centerlines using the Lorenz, Frangi and 4-step filters (see Fig. 3). As seen in Fig. 2 (right), our vessel-enhanced image behaves in a similar fashion as the other two filters by having a suppressed background and an enhanced artery. At first glance, our filter seems to maintain original coronary artery width and it seems to have less background noise when compared to the Lorenz filter. The sequential steps of preprocessing for the 4-step filter proved effective, as it did not break the continuity of the artery. To justify the importance of the four preprocessing steps for our 4-step filter, we attempted to extract the center axis using as a cost image: (i) only the homomorphic filtered image, (ii) the homomorphic and anisotropic filtered image, and (iii) the homomorphic filter coupled with shock and anisotropic diffusion image. In Fig.4, we see that the FMM was not able to cope with the cost images since an inaccurate path was extracted between the extremities of the coronary artery. It is essential to include all four steps when using our empirically

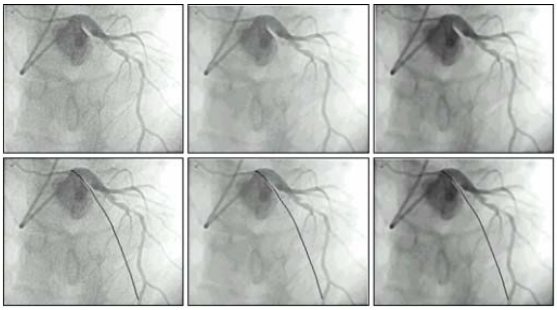

Fig. 4. (Top row) Alternative cost images using only the homomorphic filter (left), both the homomorphic and anisotropic filters (center) and the homomorphic coupled with the shock and anisotropic diffusion (right). (Bottom row) Failure of the FMM using inadequate cost images (dotted line).

found parameter values. If our disk radius for the structuring element was selected too small (<10 pixels), artery discontinuity would have resulted, especially at stenosis locations.

Lastly, Table 1 shows the results obtained in the study when comparing the automated centerline coordinates to those obtained manually. The Lorenz filter proved the more precise in 4 of the 8 images. The Frangi and 4-step filters had better average distance values in the remaining 4 images. Having resized images down to 256x256 pixels and assuming an intensifier size of 178 mm, each pixel width was about 0.695mm. In all filters, the average distance errors were less than 0.58 mm (that is the 0.83 pixel mean distance in the Lorenz filter). We were fortunate not to have many neighboring structures adjacent to our arteries during the vessel enhancement phase. If it were the case it may lead to wrong trajectories in the FMM due to possible strong filter responses. Two disadvantages of our proposed filter are that some of the smaller arteries will be lost and remain unseen and we also have more filter parameters to optimize than the Lorenz and Frangi filters.

IV. Conclusion

A preliminary approach towards the automatic extraction of relevant images and the principal coronary artery centerlines has been proposed. Further work needs to be made in determining a more robust algorithm to localize the systolic image frames in our angiographic sequence. The 4-step filter successfully enhanced the principal arteries and we believe that by optimizing parameter selection we can arrive at a stable and reliable filter like the ones proposed by Frangi and Lorenz.

	Lorenz		Frangi		4-step Filter	
Image	mean	std	mean	std	mean	std
1	0,50	0,31	0,42	0,29	0,58	0,41
2	0,83	0,54	0,81	0,52	0,62	0,40
3	0,37	0,25	0,31	0,25	0,56	0,27
4	0,48	0,27	0,63	0,43	0,70	0,60
5	0,64	0,83	0,77	0,76	0,55	0,34
6	0,41	0,30	0,44	0,22	0,57	0,41
7	0,37	0,34	0,45	0,36	0,60	0,46
8	0,52	0,24	0,54	0,30	0,73	0,38

Table 1. Mean distances and standard deviations from FMM to reference centerlines for cost functions based on image enhancements with the Lorenz, Frangi and 4-step filter. All values in pixels and images were resized to 256 x 256 pixels. The Lorenz filter produced a cost image that yielded a centerline that was more precise in four angiographic images, followed by both the Frangi and 4-step filters.

References

[1] American Heart Association. 2005 Heart and Stroke Statistical Update, American Heart Association. Available at: http://www.americanheart.org/downloadable/heart/1105390918119HDSStats2005Update.pdf (Accessed April 24, 2006)

[2] C. Lorenz et al.: Multi-scale Line Segmentation with Automatic Estimation of Width, Contrast and Tangential Direction in 2D and 3D Medical Images. In CRVMed-MRCAS Proceedings. Springer Verlag, 1997. p. 233-242

[3] A. F. Frangi, W. J. Niessen, R. M. Hoogeveen, T. Van Walsum, and M. A. Viergever, "Model-based quantitation of 3-d magnetic resonance angiographic images," *IEEE Trans. Med. Imag.*, vol. 18, pp. 946–956, Oct. 1999.

[4] Aylward, S., Bullitt, E.: Initialization, noise, singularities, and scale in height ridge traversal for tubular object centerline extraction. IEEE Trans. Med. Imag. 21 (2002) 61–75.

[5] O. Wink et al.: 3D MRA Coronary Axis Determination using a Minimum Cost Approach. Magnetic Resonance in Medicine 2002;47(6):1169:1175.

[6] S.D. Olabarriaga, M. Breeuwer, W.J. Niessen Evaluation of Hessian-based filters to enhance the axis of coronary arteries in CT images. CARS 2003: 1191-1196

[7] Lin, Q. PhD Dissertation. Enhancement, Extraction, and Visualization of 3D Volume Data. Institute of Technology. Linkopings University, Sweden. (2003).

[8] Homomorphic filtering notes. Available at: http://debian.fmi.unis-ofia.bg/~blizzard/download/Image%20Processing/6.Image%20Enhancement%203.pdf (Accessed April24, 2006).

[9] P. Perona and J. Malik. Scale-space and edge detection using anisotropic diffusion. IEEE Transactions on Pattern Analysis and MachineIntelligence, 12(7):629-639, (1990).

[10] G. Gilboa, N. Sochen, and Y. Zeevi. Regularized shock filters and complex diffusion. In Proceedings of ECCV, pages 399--413, Copenhagen/Denmark (2002).